Heliyon 7 (2021) e08608

Contents lists available at ScienceDirect

Heliyon

journal homepage: www.cell.com/heliyon

Research article

Harnessing of geothermal energy for a greenhouse in Ecuador employing a heat pump: design, construction, and feasibility assessment

Gonzalo Chiriboga [a,*], Santiago Capelo [a], Pablo Bunces [a], Carla Guzmán [a], Jonathan Cepeda [a], Gilda Gordillo [a], Diego E. Montesdeoca [a], Ghem Carvajal C [a]

[a] Central University of Ecuador, Chemical Engineering Faculty, Jerónimo Ritter S/N and Bolivia Quito, Ecuador

HIGHLIGHTS

- Geothermal applications are still marginal in South America.
- Tropic's temperature changes make the system shift from heating to cooling constantly.
- Geothermal conditioning of a greenhouse in the Andean region of Ecuador is feasible.
- 65% of the electricity required is used for cooling due to the COPs.
- Fuel subsidies in Ecuador make LCOH less competitive.

ARTICLE INFO

Keywords:
Geothermal conditioning
Greenhouse
Heat pump
LCOH
Ecuador
Capacity factor

ABSTRACT

Globally, the greenhouses' farming area comprises 500 000 ha, and they efficiently produce more than half of the vegetables consumed around the world. Nevertheless, high-yield crops tend to be incredibly energy-intensive. This study proposes designing and building a coupled geothermal heat pump for a 470 m^2 greenhouse in the Andean zone conditions addressing a requirement of 15 °C at night and 30 °C during the day. Firstly, the study determined the energy potential of the solar and geothermal sources employing actual measurements and contrasting the results with theoretical models. Then, it developed an energy balance in the greenhouse to size the geothermal heat pump using the vapor compression cycle. Finally, the comprehensive system was built and evaluated through the Leveled Cost of Heat (LCOH). The operation requires a potential of 29.56 and 65.76 kW for heating and cooling; this is technically feasible when running the system with a heating flow driven by an optimized temperature ramp of 1.64 °C h^{-1}. Also, the capacity factor (CF) shows that a lifespan between 12 to 14 years is required to reach acceptable LCOH when CF is as low as 0.45. Financially, it is necessary to foster customs exemptions to make it competitive versus more traditional sources such as electricity and LPG since the main components of the heat pump and the geothermal exchanger are not produced locally and represent nearly 70 % of the upfront costs.

1. Introduction

Population grows just as people living in cities; the task of feeding these urban dwellers becomes impossible without industrialized agriculture (Lambert et al., 2014). Unfortunately, that increase in productivity demands an increase in the crop's energy intensity. This research particularly aligns with the Sustainable Development Goals (SDG) 2 and 7 (United Nations, 2015) that foster equitable food production and affordable and non-polluting energy supply to drive socioeconomic desires and aspirations (Dube et al., 2019). In this sense, one in four people globally – 1.9 billion – are moderately or severely food insecure (Roxer and Ritchie, 2019), and 28 of the 30 countries with the highest percentage of malnutrition coincidentally have the lowest access to the electricity index. Those data highlight a traditional synergy between energy and traditional agriculture, either indirectly (pesticides and fertilizers) or directly (machinery and irrigation systems) (Pervanchon

* Corresponding author.
E-mail address: wgchiriboga@uce.edu.ec (G. Chiriboga).

https://doi.org/10.1016/j.heliyon.2021.e08608
Received 11 August 2021; Received in revised form 8 November 2021; Accepted 13 December 2021

et al., 2002). Modern agriculture demands even higher quality energy inputs like electricity to heat pumping, LED light supply (Hafeez et al., 2020), and automatic control (Barkunan et al., 2019).

In the pre-industrial era, agriculture could provide around 100 % of society's energy; however, now it is a high energy demander (Krausmann et al., 2008), which in turn has reduced (Gliessman, 2000) the use of other resources like soil, water, and crop cycle times increasing the sector's revenue (Chowdhury et al., 2020). Roughly 80 % of artificial energy consumed in agriculture derives from oil and natural gas used in tractors operation, harvest transport, conditioning, and drying. The remaining 20 % is electricity mainly employed in pumping and irrigation (Stout and Fluck, 1992). By 2019, the agricultural sector in Ecuador represented 8 % of the total Gross Domestic Product (GDP) and generated 2 million jobs in rural areas (Ministry of Agriculture, 2019). Its energy consumption corresponded to 1 094 kBOE, of which 18 % represents liquefied petroleum gas (LPG), whose final uses are mainly: temperature control for greenhouses and warehouses, hot water and sanitation, localized generation, drying, and carbon dioxide enrichment (Marchi et al., 2019). In the country, thermal appliances are still very fossil fuel dependent in the farming sector, although alternative technologies have been successfully employed in other countries (Hermatian et al., 2019) since those applications do not require a power source of large thermal availability or high quality (Ammar et al., 2012).

A greenhouse efficiently handles scarce resources such as carbon dioxide and sunlight. It can improve ventilation (Bartzanas et al., 2004), heating (Attar et al., 2014) or cooling (Bouadila et al., 2014), and light intensity (He et al., 2019) to accelerate the plant growth (Yang, 2021). The world greenhouse farming area is about 500 000 ha (van Rijswick, 2018), and more than half of vegetables grow in greenhouses. The top two reasons for farming undercover are extending the growing season

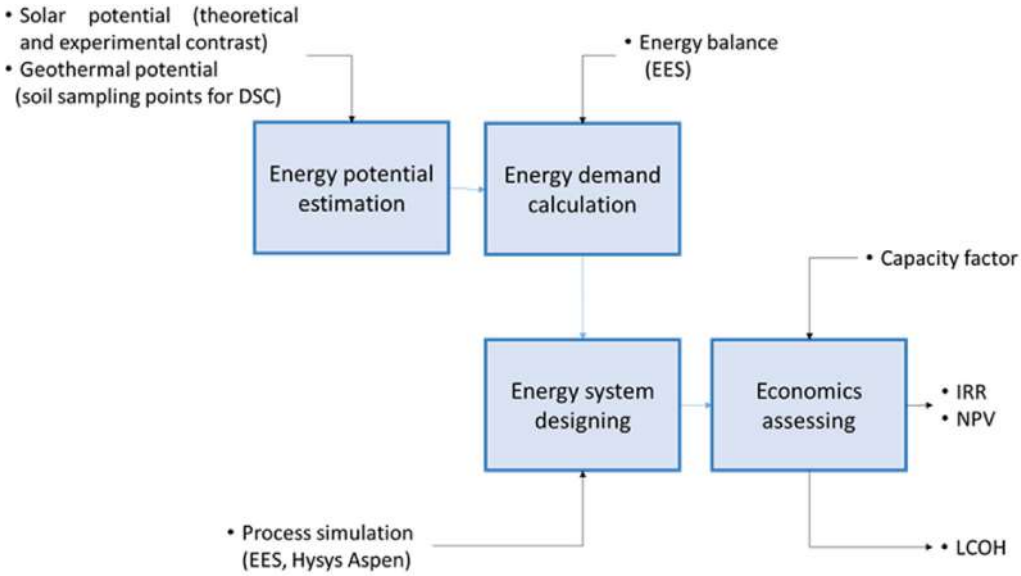

Figure 1. Relations diagram – Method depiction.

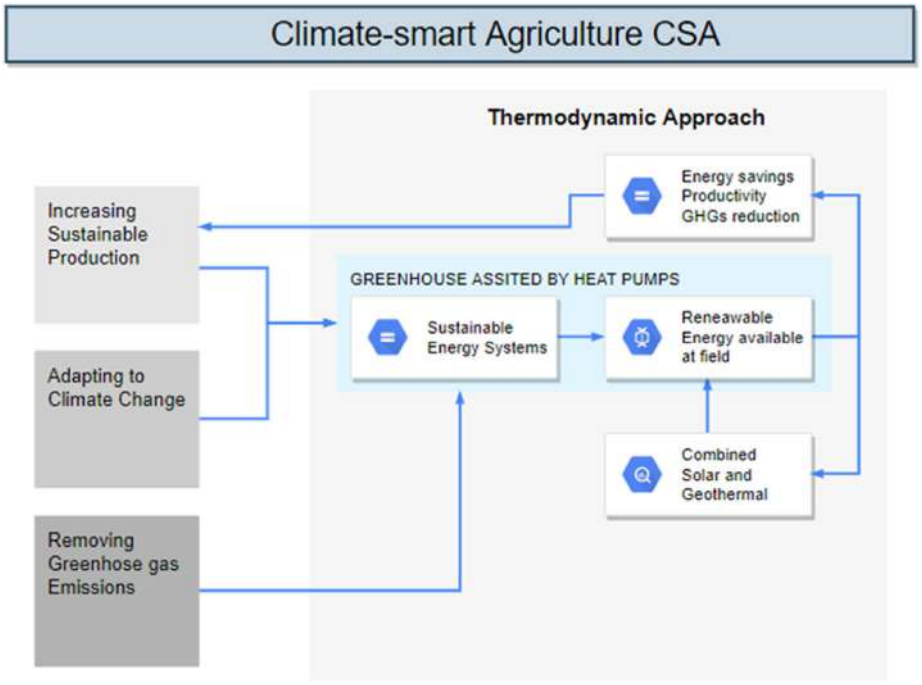

Figure 2. Project global methodology adjusted to CSA.

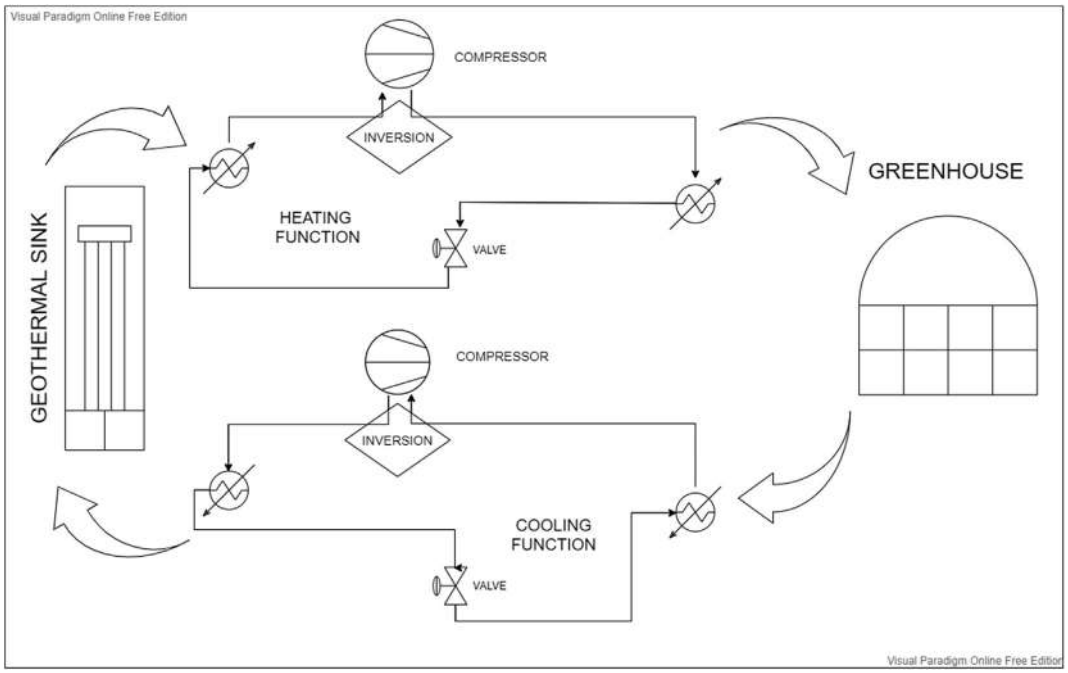

Figure 3. Heat pump and refrigeration functioning.

and transplant operation practices (Miller, 2019). In the tropics at high altitudes, greenhouses usually require heating and cooling coupled systems since temperatures variations could be significant in short periods. Those variations interfere with the reproductivity in numerous species of flowers and vegetables (Willits and Peet, 1998). As a rule of thumb, plants grown in greenhouses have adapted to average temperatures ranging from 17 to 27 °C in the daytime and 15–20 °C at night (von Zabeltitz, 2011). Unfortunately, the greenhouse selected is overwhelming out of these limits. It reaches 50 °C at noon and closes to 0 °C at night. So, farmers usually burn the gas at night to increase the temperature, making the system fossil-fuel dependent, or ventilate the greenhouse during the day to decrease the temperature, forgoing the carbon enrichment (Yasutake et al., 2017).

Few studies have pointed out the difficulties associated with the conditioning of a greenhouse in the Andean zone with high levels of solar radiation, non-seasonal extreme conditions, and low thermal mass of the air, which in turn causes high-temperature variability throughout the day. This climatic peculiarity provokes the system to alternate from heat pump to refrigerator over and over in short time cycles. This document explores the technical feasibility of, on the one hand, a system whose geothermal sink reduces the influence of climatic conditions; and on the other hand, the optimization of the heating and cooling cycles, using temperature gradients that continuously ensure the required energy availability.

The Ecuadorian energy market has stood out for subsidizing the price of fossil fuels, which has weakened the development of alternative

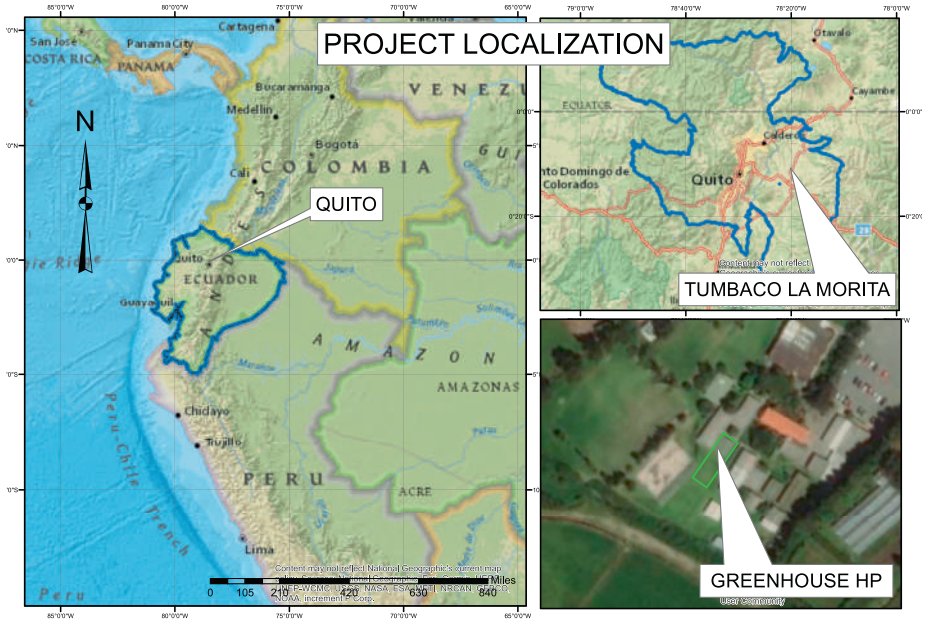

Figure 4. Project georeferencing imagery.

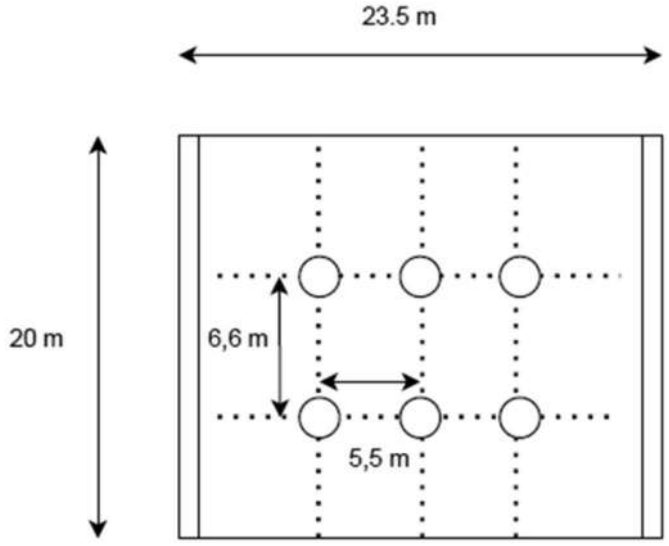

Figure 5. Soil sampling points inside the greenhouse.

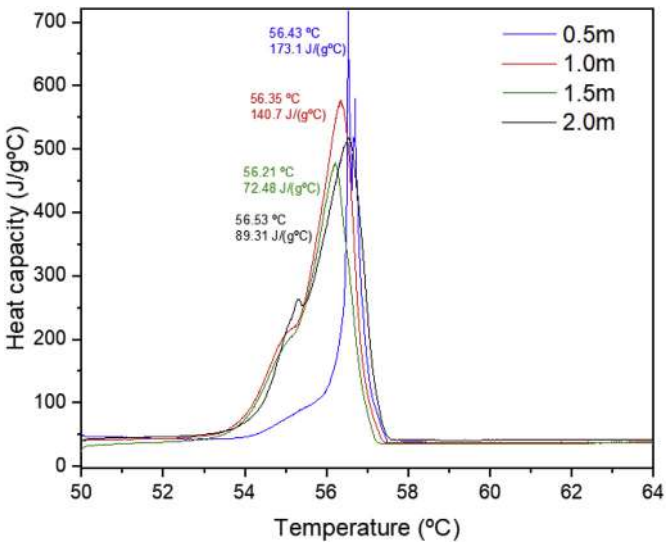

Figure 7. Differential scanning calorimetry of soil samples.

energy sources and jeopardized the national budget every year. Therefore, since 2020 the partial withdrawal of the subsidy seeks to bring the derivative prices to international levels. This fact generates a research gap in all sectors of the economy in pursuit of energy matrix diversification. This project aims to design and install the first greenhouse assisted by a geothermal heat pump in Ecuador. This facility was conceived and built by the Chemical Engineering Faculty of the Central University of Ecuador. Once in operation, it will be available for the Agricultural Sciences Faculty to develop comprehensive research that contributes to sustainable agriculture.

The project follows four phases:

1. Energy potential estimation from the two primary sources: solar radiation and the geothermal sink
2. Energy demand calculation based on an energy balance in the greenhouse and the horizontal geothermal heat pump (HGHP) determination.
3. Energy system designing endorsed by a comprehensive simulation of the entire process according to the specifications, and the construction of the system, including the geothermal reservoir
4. Economics appraising the system performance through a technical and financial analysis based on the Leveled Cost of Heat (LCOH)

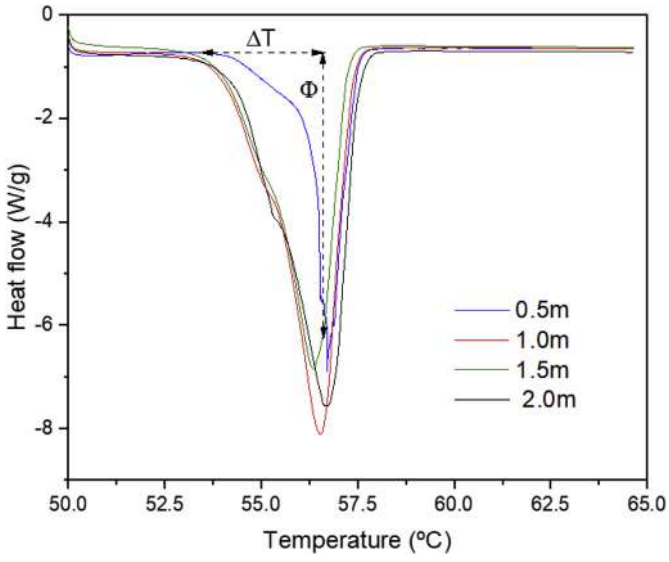

Figure 6. Thermal conductivity determination.

The document begins by describing a methodological adaptation adjusted to Ecuadorian highlands conditions following the sustainable agriculture guidelines. The next chapter contains the technical and financial analysis results, which represent the feasibility of using the low enthalpy geotherm in those agricultural greenhouses. Finally, in the last chapters, the document carried out a critical assessment of the results comparing the employment of geothermal before subsidized alternatives such as electric and fossil.

2. Methods

The following diagram describes the methodology applied to the case study. Each box represents a process with the main inputs and results. The analysis covers 4 main processes: supply and energy demand, design, and economic evaluation. The detail of the methods and materials is indicated in a timely manner in each subsection Figure 1.

Climate-smart agriculture (CSA) is an approach to reorient agricultural systems to support the development and ensure food security effectively. This study proposes a heat pump that controls the thermal conditions only; however, it is worth mentioning that the relative humidity and artificial light are drivers that will remain for our pending studies.

2.1. Case study description

Following the CSA method (Figure 2), the greenhouse's users will meet the temperature requirements employing an adapting technology.

Table 1. Greenhouse and material properties.

Parameter	Value	Unit
Material	Polyvinyl chloride	
Wall thickness	7.00	μm
Conductivity	0.16	W m^{-1} K^{-1}
Transmittance	0.91	
Absorbance	0.02	
Length	23.50	m
Width	20.00	m
Height	3.50	m

Table 2. Soil results in function of depth.

Depth [m]	Conductiviy [W m^{-1} K^{-1}]	Porosity	Density [kg m^{-3}]	Specific Heat [J kg^{-1} $°C^{-1}$]	Difusivity [cm^2 s^{-1}]	Avg Temp [°C]
1.0	0.3146	0.39	1 950	576	0.00281	17.30
1.5	0.3140	0.26	1 730	478	0.00380	17.69
2.0	0.2907	0.34	1 870	518	0.00299	19.40

(1) The coefficient of performance (COP) will quantify the replacement of fossil fuels or electricity for geothermal, (2) any sustainable energy system must prioritize sources close to the point of use to increase sustainable production. The result will be a process adapted to a type of energy that suffers very little influence from the effects associated with climate change (3). The main shortcoming of these systems is the initial investment; thus, economic indicators will evaluate performance and applicability to Ecuadorian reality.

Design features. The desired temperature and local conditions need the operation of one refrigerator during high-temperature hours that removes heat from the greenhouse and one heat pump at night when the temperature decreases. Therefore, a unique system with a reversing valve represents an attractive alternative, which will shift the system between heating and cooling mode (Figure 3). The set-point temperature is 30 °C at day and 15 °C at night.

Site description. The greenhouse area is 470 m^2; it lies in Tumbaco - La Morita, the coordinates are 0°13'41.8″S 78° 22'18.5″W, 25 km away from Quito at 2 357 m above sea level (masl) inside the Central University Campus. The climate is classified as C_{fb} by the Köppen-Geiger system. The average annual temperature is 14.3 ± 5 °C, and rainfall is 2 877 ± 315 mm y^{-1}.

2.2. Energy potential

Solar. The project is in the Andean Mountains (Figure 4), where solar radiation reaches the earth perpendicularly; on average, 12 h of sunlight are typical and independent of season. A theoretical solar radiation model was generated from January 1, 2012, to October 6, 2018, following the methodology described by (Duffie and Beckman, 2013) that considers the light hours, slope, and sky type according to the geographic point. For contrasting the model, measurements of effective solar radiation were taken directly with the LSI-LASTEM DPA053 Sensor Class 2 OM thermopile type 0 to 2000 ± 10 W m^{-2}. In addition, a meteorological station collected data on global solar radiation, temperature -20 to 80 ± 0.1 °C, wind speed 0 to 60 ± 0.07 m s^{-1}, and relative humidity 0 to 100 ± 0.1% during August and September 2018. The data were acquired in the LSI-LASTEM ELO 105 Data Logger using 3DOM® software.

Geothermal potential. The heat flow depends on the thermal properties of soil, water content (Garat et al., 2015), soil temperature, and the exchange area. The project proposes a horizontal linear loop exchanger to harness land availability (Cui et al., 2019). The sampling followed the Unified Text of Environmental Legislation of Ecuador (TULSMA) method shown in Figure 5; the soil temperature was measured for 4 h during day[2] and night. The depths were 0.5; 1.0; 1.5; and 2.0 m in six points simultaneously. Finally, 500 g of soil at each depth was taken to posterior analysis in the laboratory.

Once in the lab, the sub-samples will be mixed and homogenized to obtain representativeness. The gravimetric analysis determines the actual density value as well as humidity. Differential Scanning Calorimetry (DSC) METTLER TOLEDO Calorimeter Robust MultiSTAR 0.02–300 K/min ±1 % can estimate the thermal conductivity through the melting principle (Hakvoort et al., 1985) Figures 6 and 7.

Again, DSC calculated the specific heat. The total heat corresponding to the transformation produced in a sample from the thermograph (Plante et al., 2009) shows the specific heat trend.

Table 3. Fundamental energy and heat transfer equations.

Description[2]	Equation
Effective solar radiation	$\alpha + \tau + \delta = 1$
Heat transfer coefficient	$k_h = \frac{1}{\frac{1}{h_i} + \frac{e_c}{\lambda_c} + \frac{1}{h_e}}$
Heat flow greenhouse - environment	$Q_h = k_h \times (t_e - t_i)$
Heat flow greenhouse - soil	$Q_s = k_s \times \frac{(t_s - t_i)}{h}$
Heat flow required	$Q_a = Cp_a \times (t_{sp} - t_i)$

2.3. Energy demand

The demand relies on an energy balance that considers the actual temperatures inside the greenhouse (Anifantis et al., 2016) and the thermal requirements specified for each crop (Obara et al., 2011).

$$R_n + Q_{hp} = Q_h + Q_a + Q_s \quad \text{Eq. 1}$$

The transmitted radiation (R_n) and the heat energy produced by the heat pump system ([1]Q_{hp}) correspond to energy inputs and the heat lost by conduction and convection through the material (Q_h), the sensible heat required to reach the set-point (Q_a), and the heat flux lost by conduction through the ground (Q_s) depend on the continuous shift of energy potential driven by local conditions. The heat fluxes related to the biological respiration of plants and evapotranspiration are minimal compared to solar radiation, so the balance excluded them from the analysis. It does not consider either ventilation for avoiding the reduction of carbon dioxide enrichment.

Additional information from the meteorologic station, materials specifications, and photosynthesis requirements listed in Table 1 were introduced in the Engineering Equation Solver (EES) to solve the energy balance. The Air-ha thermodynamic package (Lemmon et al., 2000) and the Heat Transfer Library (Nellis and Klein, 2009) were selected.

2.4. System design

Real operating conditions defined the thermodynamic cycle, i.e., evaporator overheating by 6 °C (Pu et al., 2018), a compressor efficiency of 90 %, and a subcooling of 5 °C in the condenser. Then EES's max/min function identified the maximal COP corresponding to the minor work required for the heating or cooling. The software evaluated five refrigerants available in the local market: R134A, R404A, R410A, R600A, and R290; a pipe of high-density polyethylene was selected according to (IGSHPA, 2016); the selection of central units is based on fluid information and the thermodynamic properties (ASHRAE, 2018). LOGOSoft Comfort® was used to program the logic controller. Finally, Aspen Hysys® simulated the entire coupled system. Since this software has no four-way valve for cycle inversion, heating and cooling simulations are carried out separately.

[1] Qhp or Qr are used when the system works as a heat pump or refrigerator, respectively.

[2] The data are collected and loaded to the software.

Table 4. Effective solar radiation and extreme temperatures in the greenhouse.

Parameters	Value	Unit
Effective radiation	3.6	MJ m^{-2}
Registered maximum temperature	45.2	°C
Registered minimum temperature	4.0	°C

2.5. Economic assessment

Geothermal typically has high upfront investments for the heat pump system and the excavation; nevertheless, the operation is relatively low. Therefore, this study considered a lifespan assessment method. It starts from a cash flow, including the equipment's costs, civil works, excavation and heat exchanger, water supply and treatment, electricity, labor, and reconditioning of the greenhouse. The Central Bank of Ecuador established the effective rate for the productive business as a reference (Goldstein and Hiriart, 2012a) with a linear depreciation of 10 years. The analysis used the current tax table in Ecuador for services contracting and maintenance; the electricity and LPG costs are public information from the Electricity Regulation and Control Agency and the Petroecuador Public Company. Cash flows follow the methodology of fundamental capital budgeting (Berk and DeMarzo, 2017). First, the calculation determined the IRR and NPV of the project and varied the interest rates to evaluate incentives for capital use. Second, it estimated the leveled cost of heat (LCOH) with a capacity factor of 1. For temperate latitudes, this value ranges from 0.20 to 0.35 (Goldstein and Hiriart, 2012b). Nonetheless, the temperature variability in the tropics would increase the capacity factor because of the simultaneous heating and cooling demand, although there is very little published information in this regard. Here, the research rehearsed the LCOHs as a function of capacity factor, ranging from 0.20 to 0.60.

3. Results

Initially, Table 2 reports the laboratory results of the geothermal sink; meanwhile, Tables 3 and 4 indicate the fundamental heat transfer equations and the solar energy parameters, respectively. All these inputs permit determining the energy potential and the heat losses.

The sink temperature increases with depth; however, properties such as conductivity decrease and porosity increase. These facts influence the heat transfer in different ways, so a response surface optimization determined a depth of 2.4 m to favor heat exchange in the geothermal sink. Next, the analysis compares the average temperatures measured inside the greenhouse (from August to September 2018) with those at different soil depths (1.0, 1.5, and 2.0 m). it also includes the temperature desired by the farmer according to the specific crop requirement. It is worth mentioning that this temperature could change in case of migrating to another type of crop. In this case, the system requires a maximum temperature of 30 °C, at day and 15 °C at night ±2 °C. A temperature ramp of 5/3 °C h^{-1} to determine the electricity consumption, this assumption will allow reaching a steady-state operation progressively.

Figure 8 indicates the most critical intervals for heating from 24:00 to 08:00 and for cooling from 10:00 to 15:00. (a) Shows the heating mode mainly during the night, (b) represents the cooling mode at midday, (c) shows the global system in an entire day. The conditioning system seeks to even the blue bars with the dots. The system will turn off at 9 am and 3 pm because solar radiation and heat losses would only reach the set-point. Note how the ramp is applied to harness the thermal mass and reduce the energy consumption. However, the system does not depend solely on the input or output energy but also on the transfer capacity, driven by the temperature differential.

In tropical countries, the presumption that the ground-source heat pump may not provide good thermal arises because the difference between ground and atmospheric temperatures is essentially low (Widiatmojo et al., 2019) does not come into play for Andeans. The system has a peculiarity inherent to the area's climatic conditions, and the temperature depends strongly on the presence of solar radiation, so it continuously works like a refrigerator, heat pump, or turns off to meet the thermal objective. Under these conditions, a gradual temperature change is proposed with an optimized ramp whose objective function is to minimize the events in which the temperature difference between source and sink compromises the achievement of the thermal objective Figure 9.

This figure compares the main temperature differentials and shows the hour when each event occurs. Points under line 1:1 mean the differential between the actual and desired temperatures in the greenhouse are higher than the differential in the reservoirs. Next, the function Max/Min in EES finds an optimized ramp of 1.64 °C h^{-1} to procure higher availability and harness the heat stored in air mass. Finally, the primary energy flows that drive the energy balance inside the greenhouse are obtained.

Effective solar radiation consists of absorbance (α), transmittance (τ), and reflectance (δ). The convection coefficient of the greenhouse outdoor and indoor are given by (he) and (h_i) respectively (t_i) represents the internal temperature of the greenhouse (λ_c) the thermal conductivity of the covering material, and (e_c) the thickness of the material. Finally, the specific heat of the air (Cp_a) and the set-point temperature (t_{sp}) will determine the heat flow required to size the energy system. The outcome for heating and cooling requirements to meet the set-point are 29.56 and 65.76 kW, respectively.

Hereafter, EES determined the state variables for the refrigerant R290 in the following order: 1) inlet to the evaporator, 2) inlet to the compressor, 3) inlet to the condenser, and 4) inlet to the expansion valve. It also calculates the specific energy requirements and COP for refrigeration (r) and heating (hp) modes.

Refrigerant R290 is non-toxic but extremely flammable substance, GWP = 3, and ODP = 0. Tables 5 and 6 show the thermodynamic results, especially the COP, which means that 3.2 energy units of cooling power is achieved for each energy unit of power consumed by the pump's compressor. Table 7 indicates the results obtained for the geothermal heat exchanger and the compressor in cooling and heating modes. The overall results for the pumping system specification are sized based on the cooling mode due to the higher demand. Tables 8 and 9 depict the outcomes of the thermodynamic balance applied to the pressure devices.

Table 10 shows the results obtained for the refrigerant/water and refrigerant/air heat exchangers. The UA factor represents the global heat transfer coefficient U times the transfer area A.

To analyze the costs associated with the project, the next figure breaks down the main components purchased locally in 2020 dollars Figure 10.

The investment of $ 39 100.00 falls into year zero. Operation and maintenance costs come into force from year 1. This component covers administrative, logistics, and maintenance, which equals $ 882.00 for year one and an increase of $ 100 for subsequent years. Taxes amount to $ 471.00 per year, and they represent 12 % of contracting services and the correction for the decrease of depreciated investment. The electricity cost charged for this project fits in the medium-voltage-industrial zone with a value of 0.095 $ kWh^{-1}. These parameters allow us to estimate from year one of $ 4203.38.

Tables 11 and 12 indicate the Net Present Value (NPV) analysis considering 20 years of the project's life and the established interest rate of 9.50 %, the NPV and IRR are $ 4 564 and 11.30 %, respectively. Firstly, the capacity factor assumed is 1; however, this parameter is varied to estimate LCOH as a function of the operation time. This last analysis in

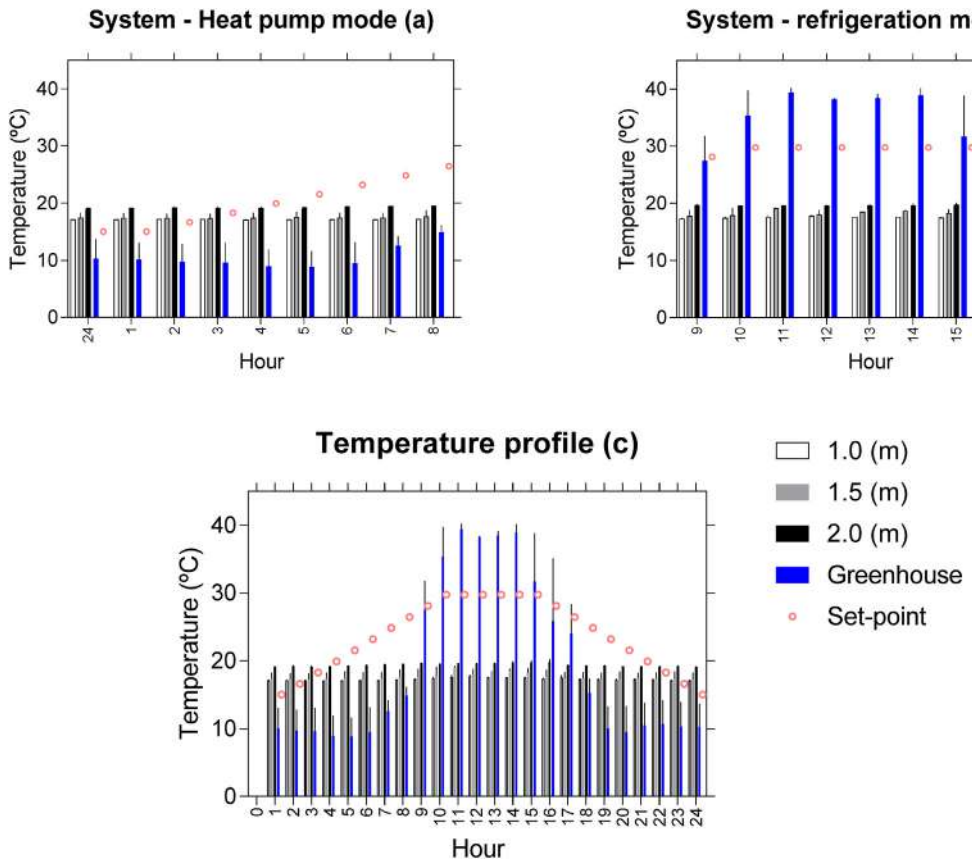

Figure 8. Temperature profiles, including soil, greenhouse, and setpoints.

Figure 11 shows the sensibility of the LCOH in the function of the capacity factor.

The values under the horizontal lines represent scenarios in which operating the heat pump has a lower LCOH than electrical resistance. For example, for a system projected for 20 years, its capacity factor should at least be 0.4; that is, ensuring a minimal 3 504 h of operation per year. However, LPG has a price of 0.057 \$ kWh^{-1} due to the fuel subsidy program that the government has maintained since the 70s.

4. Discussion

4.1. Ecuador and South American situation

In Ecuador, geothermal energy has strictly focused on the tourist bathing, therapeutic, and resort sectors; areas such as Papallacta, Baños, and Chachimbiro are popular, with an installed potential of around 5 MW. However, The country has overlooked its energy use for heat pumps or electricity generation, and there is little published information in this regard. For example, Lloret et al. reported a total geothermal potential of 3000 MW, mainly useable in high and medium enthalpy electricity generation, although they mention the importance of venturing into geothermal for conditioning (Lloret and Labus, 2014). The most studied areas turn out to be Tufiño-Chiles, Chalcana, Chalupas, Chachimbiro, and Alcedo in Galapagos due to their proximity to volcanic sources (Beate and Urquizo, 2015) (Lahsen et al., 2015). The use of geothermal energy in the entire South American context could be marginal since, to our knowledge, only one 48 MW plant is generating electricity in Cerro Pabellón Chile (Enel Generación Chile, 2017), which in 2019 produced 201 GWh (OLADE, 2020). This small deployment of geothermal could be due to the leveled cost of electricity and the cumulative capacity of hydropower and natural gas (Yao et al., 2021).

In addition to our operating project, the National Institute for Geological and Energy Research (IIGE) started construction of a greenhouse powered by a heat pump, which will warm the air inside the greenhouse when ambient temperatures fall under 12 °C; however, lateral windows ventilation will address the cooling requirements during the day instead of an inversion valve system (Beate et al., 2021). At the regional level, few studies have focused on geothermal systems, either for power generation at low temperatures (Christiansen et al., 2021), as well as heat pumps (Garat et al., 2015), critical design parameters (Maripangui et al., 2016), potential estimations (Santos et al., 2016) or as an alternative to firewood burning to heat homes in Coyhaique (Maripangui et al., 2016). In the specific case of geothermal for greenhouses, users still do not fully understand its application and benefits (Payera, 2018), and there is much uncertainty regarding the initial investment. Therefore, few projects are operating permanently in the region, for example, Chile reports two projects the first is a horticultural greenhouse with a power of 165 kW located in Lampa Metropolitana, and the second is in Puerto Aysén where a heat pump system warms a greenhouse of 150 m^2 struggling with the complex conditions of La Patagonia (Ministerio de Energía, 2017). Argentina boasts a 40.10 TJ y^{-1} project, as reported in the World Geothermal Congress 2020 (Lund and Toth, 2021). In respect of Ecuador, only technical feasibility studies have been carried out (Bunces, 2017; Capelo, 2017; Guzman, 2019; Instituto de Investigación Geológico y Energético, 2019), leaving aside the financial assessment, so this document presents the first comprehensive analysis of an operating system in the country.

4.2. System performance

Our system consists of a 470 m^2 greenhouse operating with the R290 refrigerant accepted in Ecuadorian legislation for its ozone depletion potential value; two optimizations were carried out based on the cost-benefit of the excavation depth and the cooling and heating ramp depending on the available temperature differential. The system has a maximum capacity of 29.65 and 65.76 kW to heat and cool the system,

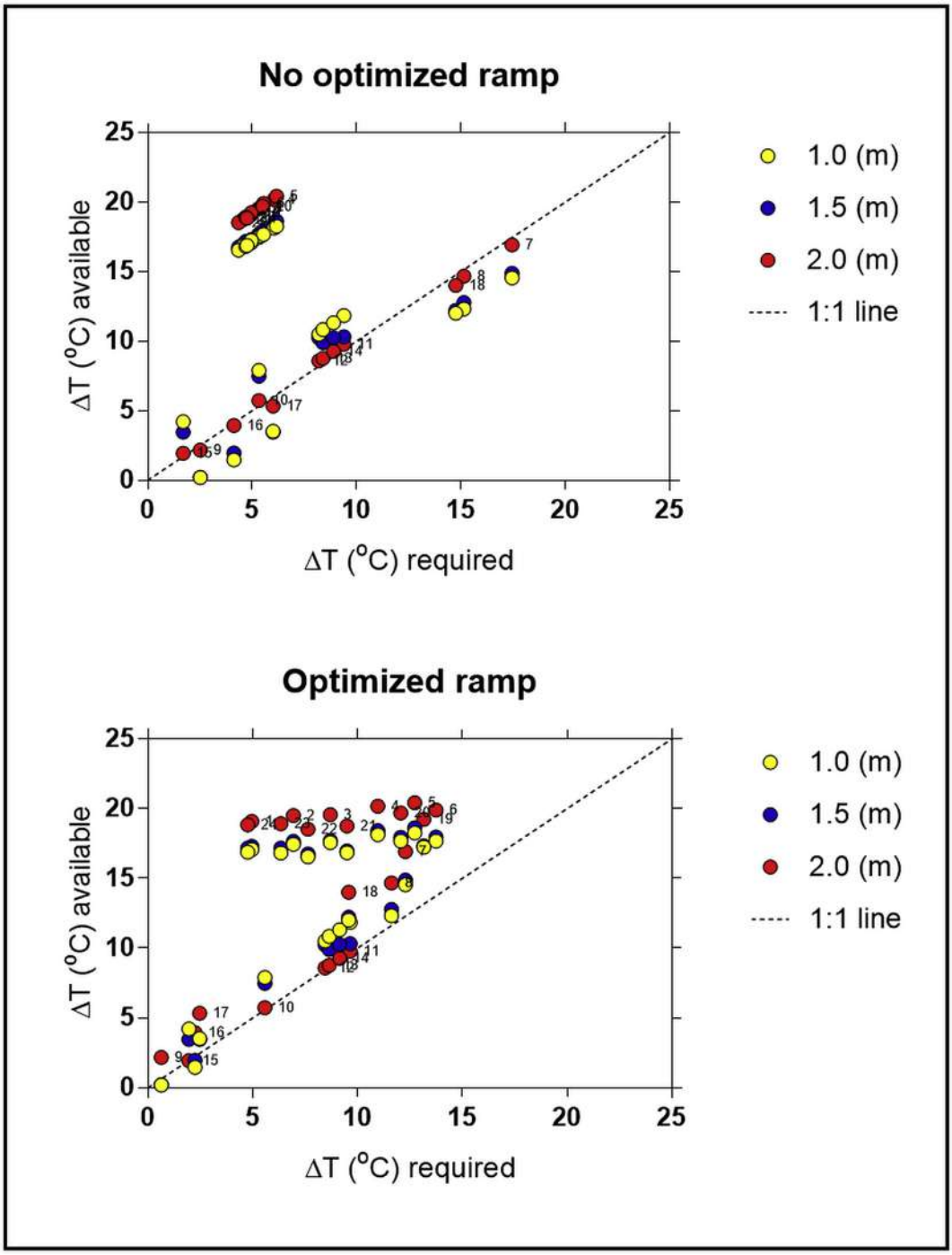

Figure 9. Optimized conditioning ramp of temperature.

respectively. It is coupled to a 526 m linear loop geothermal heat exchanger to take advantage of the vast area available in the sector and better thermal performances (Pu et al., 2018), buried at a depth of 2.4 m, also avoiding possible effects of solar radiation and shadow on the surface of the exchanger (Li et al., 2019). Electricity consumption will be 59.30 kWh d^{-1} (21.04 and 38.26 for heating and cooling, respectively). Refrigeration has the most significant participation with 65 %. The working fluid is R290 with a flow between 0.09 and 0.29 kg s^{-1} and a

Table 5. Thermodynamics solution of refrigeration cycle.

	Enthalpy [kJ kg^{-1}]	Pressure [kPa]	Entropy [kJ kgK^{-1}]	Temperature [°C]	Q_{hp} [kJ kg^{-1}]	Q_r [kJ kg^{-1}]	W_R [kJ kg^{-1}]	COP_R
1	350.7	519.5	1.546	3.0		238.1		
2	588.8	519.5	2.407	9.0			74.5	3.2
3	663.3	2 089.0	2.429	72.9	312.6			
4	350.7	2 089.0	1.491	54.4				

Table 6. Thermodynamics solution of heating cycle.

	Enthalpy [kJ kg^{-1}]	Pressure [kPa]	Entropy [kJ kgK^{-1}]	Temperature [°C]	Q_{hp} [kJ kg^{-1}]	Q_r [kJ kg^{-1}]	W_R [kJ kg^{-1}]	COP_R
1	308.4	519.5	1.393	3.0		280.4	58.4	4.8
2	588.8	519.5	2.407	9.0				
3	647.2	1 543.0	2.425	57.6	338.8			
4	308.4	1 543.0	1.362	40.3				

Table 7. Geothermal heat exchanger results.

Description		Value $_r$	Value $_{hp}$	Unit
Flow	Friction losses	851	285	kPa
	Outside area	49.6	49.6	m^2
	Cross-sectional area	7.07×10^{-4}	7.07×10^{-4}	m^2
	Flow	1.46×10^{-3}	8.81×10^{-4}	$m^3\ s^{-1}$
	Mass flow	1.45	8.79×10^{-1}	$kg\ s^{-1}$
	Speed	2.06	1.25	$m\ s^{-1}$
	Length	5.26×10^2	5.26×10^2	m
Pumping	Power	1.24×10^3	2.51×10^2	W
Heat	Reynolds	9.40×10^4	3.62×10^4	
	Prandtl	4.32	7.31	
	Nusselt	5.44×10^2	2.41×10^2	
	Convection coefficient	1.14×10^4	4.74×10^3	$W\ m^{-2}\ °C$
	Global Transfer coefficient	2.03×10^2	1.98×10^2	$W\ m^{-2}\ K^{-1}$
	Logarithmic mean temperatures	-9.01	2.52	°C
	Total heat removed	-9.07×10^4	2.47×10^4	W

compressor power of 21 kW. The coefficients of performance are 3.2 and 4.8 for refrigerator and heat pump, respectively. Our results are consistent with (Nem and Nem, 2018), who report an average of 29 kWh d^{-1} to heat a 420 m^2 greenhouse built with two layers of glass and an air separation that significantly reduces heat losses. (Noorollahi et al., 2016) indicate a consumption between 843 and 998 kWh d^{-1} for a greenhouse of 4 360 m^3 and 1 000 m^2; it is important to note that consumption is nine times higher than our system per unit area due to the extreme stational conditions (Alborz - Iran). Small greenhouses show better yields per unit area(Anifantis et al., 2016; Boughanmi et al., 2018). In short, greenhouse material, seasonality, and radiation would are the highest electrical-consuming drivers. So integral modeling addressing those factors is advisable before building a system. A comprehensive guide is provided by (Cui et al., 2019).

4.3. Geothermal perspectives in Ecuadorian agro-industrial sector

Agricultural products grown with high yields tend to be amazingly energy-intensive (Hall et al., 2000). Some studies have been carried out in Ecuador to quantify energy demand for crops focused on biofuels (Chiriboga et al., 2020). However, a disaggregated analysis of the type of energy consumed by each crop for fruits and vegetables would be necessary to better evaluate this sector's energy diversification. These outcomes would allow us to identify the most efficient primary energy

Table 9. Valve operation conditions.

	Pressure [kPa]		Temperature [°C]		Flow [kg/s]	
	Min	Max	Min	Max	Min	Max
Inlet	1 543.0	2 083.0	40.3	54.4	0.09	0.29
Outlet	519.5	519.5	3.0	3.0		

type for each application. In a study developed in the European Union addressing the changes in energy consumption in agriculture, two conclusions emerged 1) a gradual diversification of energy is evident because of the increase of renewables and electricity participation 2) and the increase in renewables is closely related to the economy's parameters (Ferrari and Zanotto, 2021). This replacement was observed mainly for gaseous fuels (heat applications), while the consumption of liquid fuels (mechanical applications) has not altered significantly, this is due to the type of transformation that energy must follow to become functional. In this sense, heat is useful directly without a thermodynamic cycle, avoiding the respective energy losses. From this point of view, geothermal becomes interesting. Globally the employment of renewables in farming is adapted from previous experiences in other sectors such as residential, commercial, and industrial. Unfortunately, in Ecuador, both the fuel subsidies policy and the government's exclusivity of the energy supply have not allowed the generation of the economic incentive or the legal scenarios for renewables to develop in other sectors where their implementation represents a lower risk.

The latest energy balance of Ecuador reports that the entire agricultural, livestock, and aquaculture sectors consume annually 196 kBOE of LPG. They intended LPG mainly for greenhouse heating, warm water supply (aquaculture), and space conditioning, which means heat-type energy. On the other hand, the proportion of fossil fuel concerning electricity in the agricultural and livestock sectors is 12.3 (Ghisellini et al., 2016). Therefore, it is easy to estimate a potential market for

Table 10. Heat exchangers properties and results.

			Cold flow	Hot flow	Cold flow	Hot flow
Temperatures [°C]	Refrigeration	Inlet	33.0	72.9	3.0	42.5
		Outlet	48.0	54.5	9.0	30.0
	Heating	Inlet	3.0	29.0	4.0	57.6
		Outlet	9.0	22.0	15.0	40.3
Capacity [kW]	Refrigeration		90.7		69.1	
	Heating		24.7		29.8	
UA [W $°C^{-1}$]			4 961.4		3 117.7	

Table 8. Compressor parameters and working conditions.

	Pressure [kPa]		Temperature [°C]		Flow [kg s^{-1}]		Power [kW]	
	Min	Max	Min	Max	Min	Max	Min	Max
Suction	519.5	519.5	9.0	9.0	0.09	0.29	5.15	21.61
Discharge	1 543.0	2 089.0	57.6	72.9				

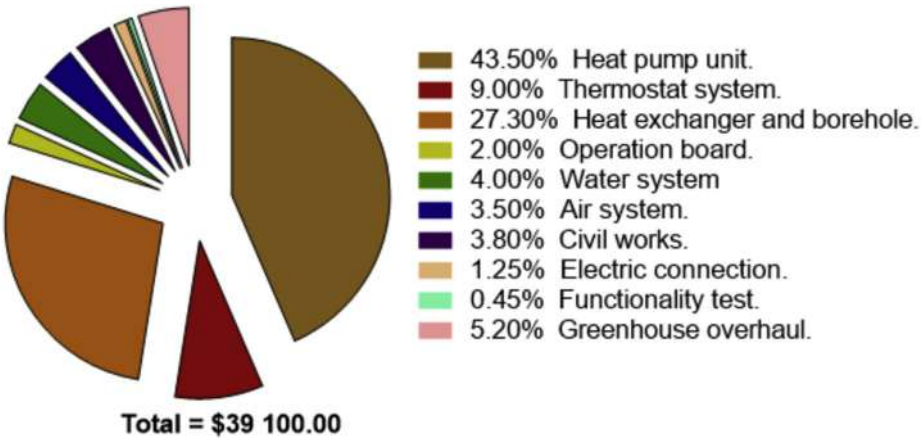

Figure 10. Disaggregated costs of the system.

Table 11. Net present value.

NPV [$]	Rate [%]
21 228	5.00
16 684	6.00
12 681	7.00
9 142	8.00
6 002	9.00
4 564	**9.50**
0	11.30

Bold denotes the actual capital cost at which these projects are financed in Ecuador.

Table 12. LCOH compared with electricity price.

Year	Capacity Factor CF					
	0.35	0.40	0.45	0.50	0.55	0.60
9	0.160	0.143	0.130	0.119	0.110	0.103
10	0.148	0.132	0.120	0.110	0.102	0.095
11	0.139	0.124	0.113	0.104	0.096	0.090
12	0.131	0.117	0.107	0.098	0.091	0.085
13	0.125	0.112	0.102	0.094	0.087	0.082
14	0.119	0.107	0.097	0.090	0.084	0.078
15	0.114	0.103	0.094	0.086	0.081	0.076
16	0.110	0.099	0.090	0.084	0.078	0.073
17	0.107	0.096	0.088	0.081	0.076	0.071
18	0.103	0.093	0.085	0.079	0.073	0.069
19	0.100	0.090	0.083	0.077	0.072	0.067
20	0.098	0.088	0.081	0.075	0.070	0.066

geothermal systems in Ecuador, in a general way, and propose a diversified energy mix[3].

The units of energy flows are kBOE; the graphs depict an evident diversification of the mix where electricity plays a central role. For example, replacing the LPG would require 155.2 kBOE geothermal annually with an increase in electricity of 40.8 kBOE. This amount would be equivalent to 0.2 % of the national energy matrix.

[3] Interest rate defined by Central Bank for these projects available at, https://contenido.bce.fin.ec/docs.php?path=/documentos/Estadisticas/SectorMonFin/TasasInteres/Indice.htm. The results are showed in 2020-American-dollars.

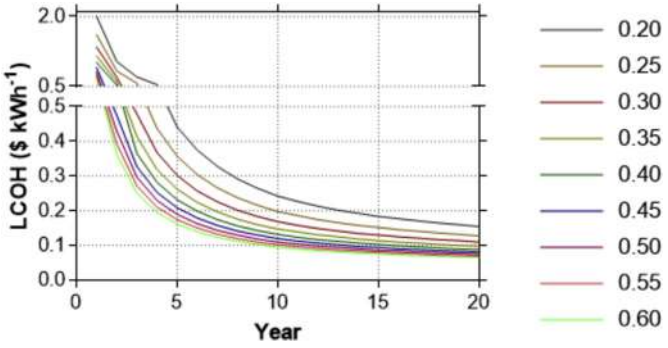

Figure 11. LCOH as a function CF.

It is necessary for a critical analysis that comprehends the increase in yields and revenues to assess geothermal completely. Figure 12 shows the most common products in the country that could be grown in greenhouses, their yields, and marketing prices. Data are available at the Ecuadorian Agricultural Public Information System (SIPA). Among the vegetables most produced in greenhouses are onions and tomatoes that add up to 81 614 T y^{-1} and an approximate market of $ 30 million y^{-1}. However, generating more disaggregated information into segments such as fruits is necessary because this sector is 11 times greater than vegetables and represents better margins for farmers. In the same way, it is essential to extend the feasibility studies to non-food markets such as flowers, which are produced exclusively in greenhouses. In 2019, this industry reached 544 million dollars in exportations, and this market is less scattered (72 % of these ventures are formal), this sector is more prone to innovate its productive processes.

4.4. Economical approach

The financial approach relies on the opportunity cost between geothermal energy and other sources such as electricity and gas; however, its implementation in different sectors such as industrial or agricultural needs detailed analysis that indicates the cost-benefit between the investment and the increase in productivity. Therefore, this study considers some key drivers that would become these projects attractive economically.

Upfront Investment. As mentioned by (Long et al., 2016) CSA, technological innovations could result in high upfront costs and overly long return of investment (ROI) periods. For example, the heat pump and the geothermal exchanger pay 40 % of their commercial value as importation charges. Tax exception and tariff preference incentives could improve, in the best scenario, the ROI in 4 years.

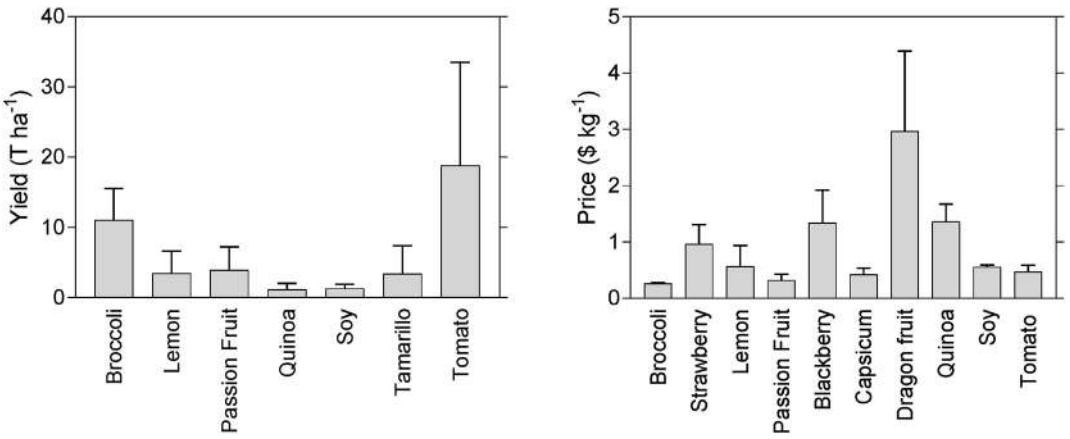

Figure 12. Yield and trading prices of greenhouse's cultivable crops.

Finally, it is crucial to have access to cheaper capital/investment; thus, a novel finance raising strategy in the country should establish interest rates in the same order as social concern housing, it is to say around 5 %. In this sense, green bonds are an alternative. Nevertheless, this project should comply and intense auditory to qualify as a credit holder, and the program has been poorly broadcasted. In 2019 the Pichincha Bank issued 30 000 credits valued at $ 150 million; so far, only big companies benefit from these bonds. The international investors who purchased these securities were the Inter-American Development Bank, the International Finance Corporation (IFC) of the World Bank.

System operation. The fuel price drives the operation costs, as happens in all energy systems. Our project uses electricity that competes with fossil fuels (subsidized). For instance, the price of LPG for household duties is the lowest in all Latin America at $ 0.11 kg^{-1}. Due to the lack of control, this fuel migrates to other sectors like industrial and agriculture putting aside renewable heating alternatives like geothermal or solar. This subsidy policy provokes serious economic issues every year since it usually expends 4 % of GDP to meet the internal demand (Chiriboga et al., 2020). Fossil fuels cannot sustain the cooling system unless they go through a thermodynamic cycle of electricity generation. In this sense, the geothermal heat pump shows the best performances, even superior to the heat pump with an atmospheric sink (Goldstein and Hiriart, 2012a). So, its implementation becomes much more attractive for cooling applications, reducing the financial analysis to the opportunity cost of

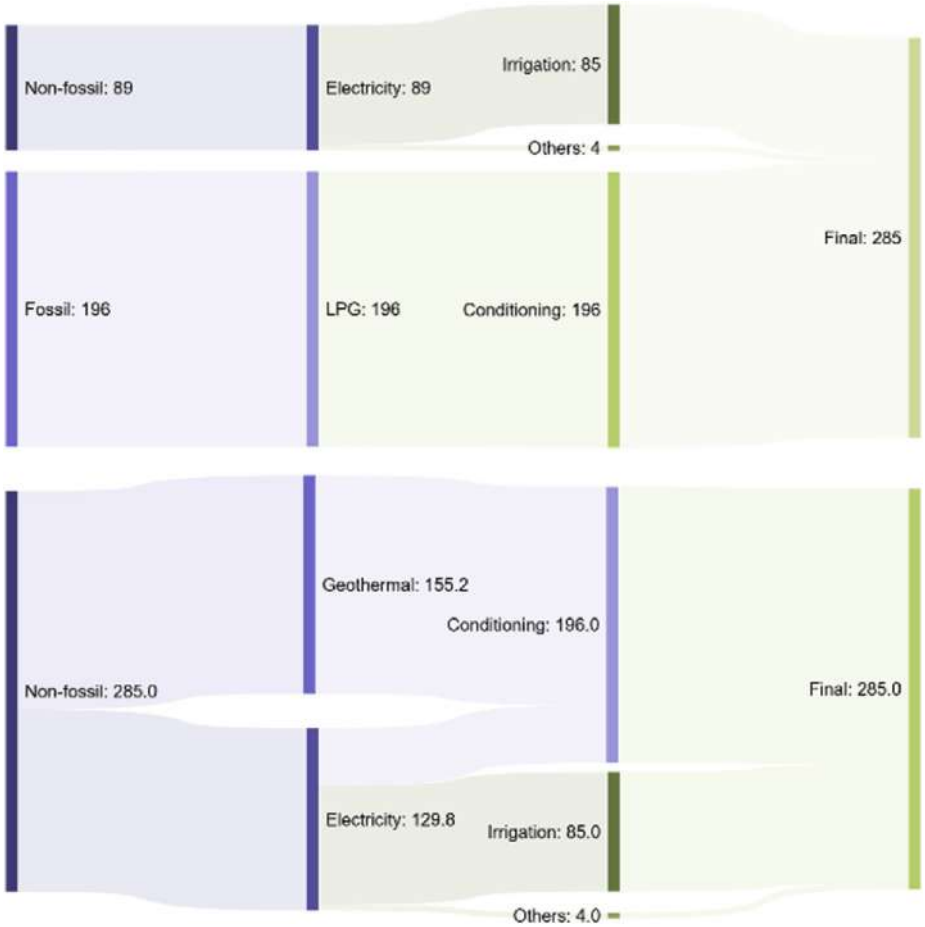

Figure 13. Geothermal heat pumps perspectives.

geothermal exchange versus the savings in electricity. Therefore, new perspectives emerge in residential and commercial conditioning facilities.

Financial indicators. The system costs \$ 0.11 kW^{-1}, consistent with the "Summary for Policymakers of 2012″ IPCC report. Likewise, they present LCOH for greenhouses coupled to a geothermal pump between \$ 0.14 and 0.287 kW^{-1} (Goldstein and Hiriart, 2012a). Figure 11 compares these data with our results at close interest rates. At least a capacity factor of 0.35 is required to achieve this range in the first 5 years. For lower capacity factors, the time can double. Our most precise analysis applied to the Ecuadorian reality indicates that the current operating conditions would hardly provide a financial advantage for this project since a capacity factor of 0.72 is required to reach a balance point between an electric heating option and the heat pump. This value is higher than generally reported for these systems; nevertheless, few systems operate in the tropics and none in Andeans. Therefore, more research in this respect, essential modifications to public policy, and cost of capital reductions are required. These measures are more plausible in the Ecuadorian context because their application does not incur a high political detriment, as does a policy against the subsidy of fossil fuels.

5. Conclusions

The high enthalpy geotherm has not been developed in Latin America mainly due to the presence and low costs of other energy sources such as hydroelectric power and natural gas. However, as the case under analysis, the low enthalpy geotherm has a more significant potential for application in this area due to the stability of the energy sink and the high requirement for conditioning of residential and industrial spaces.

The study is novel in the Ecuadorian context using geothermal energy in heat pumps. It is also one of few dealings with tropical conditions in highlands with very marked climatic variations, high levels of solar radiation, and low thermal mass of the air, which in turn causes high-temperature variability in short ranges throughout the day; this climatic peculiarity provokes the system to alternate from heat pump to refrigerator over and over continuously. Nevertheless, the system's heating (29.56 kW) and cooling (65.76 kW) capacities are sufficient to reach the set-point conditions determined (Figure 8) by the requirements of the crops most frequently farmed in the greenhouse, which makes the project technically feasible.

The analysis derived from the energy balance of Ecuador (Figure 13) allows concluding that the maximum penetration of geothermal energy in the agricultural, livestock, and aquaculture sectors, mainly for conditioning uses, is currently 155.2 kBOE per year. However, a more detailed analysis of the diversification of the energy matrix in the agricultural sector should consider the crops and the details of the different energy sources available for conditioning uses.

Financially, the project investment amounts to \$ 39 100, the LCOH, considering 20 years and an interest rate of 9.5 %, is \$ 0.097 $kW\,h^{-1}$. This cost is higher than the electricity \$ 0.095 and LPG 0.057 kWh^{-1} for the agricultural sector. The feasibility depends mainly on tax and tariff incentives and greater penetration of technology in the market, possibly in sectors less sensitive to this type of investment, such as residential and commercial. Finally, the results show that the economic feasibility of this technology depends mainly on the capacity factor derived from the type and volume of crop production. The Ecuadorian reality requires a capacity factor of 0.72 to reach similar numbers of an electric heating option.

Declarations

Author contribution statement

Gonzalo Chiriboga: Conceived and designed the experiments.

Santiago Capelo, Pablo Bunces & Carla Guzmán: Performed the experiments.

Jonathan Cepeda: Contributed reagents, materials, analysis tools or data.

Gilda Gordillo: Analyzed and interpreted the data; Wrote the paper.

Diego E. Montesdeoca & Ghem Carvajal C: Analyzed and interpreted the data.

Funding statement

This work was supported by the Research Direction (Project Senior No. 28).

Data availability statement

Data associated with this study has been deposited at the Repositorio digital - Central University of Ecuador at the accession URL: http://www.dspace.uce.edu.ec/browse?type=author&value=Chiriboga+Gavidia%2C+Washington+Gonzalo.

Declaration of interests statement

The authors declare no conflict of interest.

Additional information

No additional information is available for this paper.

Acknowledgements

The authors declare a special recognition to the Faculty of Chemical Engineering and Agricultural Sciences Deans for its management and support in developing and executing the cooperation agreements.

References

Ammar, Y., Joyce, S., Norman, R., Wang, Y., Roskilly, A.P., 2012. Low grade thermal energy sources and uses from the process industry in the UK. Appl. Energy 89 (1), 3–20.

Anifantis, A.S., Pascuzzi, S., Scarascia-mugnozza, G., Science, E., Aldo, B., 2016. Geothermal source heat pump performance for a greenhouse heating system: An experimental study. J. Agric. Eng. 47 (3), 164–170.

ASHRAE, 2018. *Handbook—HVAC Systems and Equipment*. AIR-CONDITIONING and HEATING SYSTEMS. https://www.ashrae.org/technical-resources/ashrae-handbook/table-of-contents-2020-ashrae-handbook-hvac-systems-and-equipment.

Attar, I., Naili, N., Khalifa, N., Hazami, M., Lazaar, M., Farhat, A., 2014. Experimental study of an air conditioning system to control a greenhouse microclimate. Energy Convers. Manag. 79, 543–553.

Barkunan, S.R., Bhanumathi, V., Sethuram, J., 2019. Smart sensor for automatic drip irrigation system for paddy cultivation. Comput. Electr. Eng. 73, 180–193.

Bartzanas, T., Boulard, T., Kittas, C., 2004. Effect of vent arrangement on windward ventilation of a tunnel greenhouse. Biosyst. Eng. 88 (4), 479–490.

Beate, B., Urquizo, M., 2015. Geothermal Country Update for Ecuador: 2010 - 2015 Bernardo. *World Geothermal Congress 2015, April*, 14. http://www.geothermal-energy.org/pdf/IGAstandard/WGC/2010/0160.pdf.

Beate, B., Urquizo, M., Lloret, A., 2021. Geothermal Country Update of Ecuador : 2015-2020, pp. 2015–2020, 2(October).

Berk, J., DeMarzo, P., 2017. Corporate finance. In: Corporate Finance.

Bouadila, S., Kooli, S., Skouri, S., Lazaar, M., Farhat, A., 2014. Improvement of the greenhouse climate using a solar air heater with latent storage energy. Energy 64, 663–672.

Boughanmi, H., Lazaar, M., Guizani, A., 2018. A performance of a heat pump system connected a new conic helicoidal geothermal heat exchanger for a greenhouse heating in the north of Tunisia. Sol. Energy 171 (July), 343–353.

Bunces, P., 2017. Determinación del requerimiento energético dentro de un invernadero del sector florícola [Central University of Ecuador]. http://www.dspace.uce.edu.ec/handle/25000/13186.

Capelo, S., 2017. ANALISIS DE LA FACTIBILIDAD TÉCNICA DEL USO DE LA ENERGÍA GEOTÉRMICA EN LA INDUSTRIA FLORICOLA [Central University of Ecuador]. http://www.dspace.uce.edu.ec/handle/25000/12913.

Chiriboga, G., De La Rosa, A., Molina, C., Velarde, S., Carvajal C, G., 2020. Energy return on investment (EROI) and life cycle analysis (LCA) of biofuels in Ecuador. Heliyon 6 (6).

Chowdhury, T., Chowdhury, H., Ahmed, A., Park, Y.K., Chowdhury, P., Hossain, N., Sait, S.M., 2020. Energy, exergy, and sustainability analyses of the agricultural sector in Bangladesh. Sustainability 12 (11).

Christiansen, R.O., Clavel, F., Gonzalez, M., García, P.A., Ortiz, D.A., Ariza, J.P., Martinez, M.P., 2021. Low-enthalpy Geothermal Energy Resources in the Central Andes of Argentina : A Case Study of the Pismanta System, 177. Renewable Energy.

Cui, Y., Zhu, J., Twaha, S., Chu, J., Bai, H., Huang, K., Chen, X., Zoras, S., Soleimani, Z., 2019. Techno-economic assessment of the horizontal geothermal heat pump systems: a comprehensive review. Energy Convers. Manag. 191 (February), 208–236.

Dube, K., Chikodzi, D., Nhamo, G., 2019. Making SDGs work to end hunger, sustain energy, resolve climate change, and reverse biodiversity loss. In: Sustainable Development Goals for Society, 2.

Duffie, J.A., Beckman, W.A., 2013. Available solar radiation. In: Solar Engineering of Thermal Processes, fourth ed. John Wiley & Sons, pp. 43–137.

Enel Generación Chile, 2017. Generadoras de Chile. In: Capacidad Instalada. http://generadoras.cl/empresas-asociadas/enel.

Ferrari, S., Zanotto, V., 2021. Changes in Energy Consumption in Agriculture in the EU Countries, pp. 1–12.

Garat, P., Flores-aqueveque, V., Vargas, G., Rebolledo, S., Sepúlveda, S., Daniele, L., Morata, D., 2015. Estimating low-enthalpy geothermal energy potential for district heating in Santiago basin e Chile, 76, pp. 186–195 (33.5 S).

Ghisellini, P., Setti, M., Ulgiati, S., 2016. An application of life cycle energy and cluster analysis. Environ. Dev. Sustain. 18 (3), 799–837.

Gliessman, S., 2000. Agroecology, first ed. CRC Press.

Goldstein, B., Hiriart, G., 2012a. Chapter 4 - geothermal energy. In: IPCC Special Report on Renewable Energy Sources and Climate Change Mitigation. IPCC, pp. 401–436. http://srren.ipcc-wg3.de/report/IPCC_SRREN_Ch04.pdf.

Goldstein, B., Hiriart, G., 2012b. Chapter 4 - geothermal energy. In: IPCC Special Report on Renewable Energy Sources and Climate Change Mitigation. IPCC, pp. 401–436.

Guzman, C., 2019. DISEÑO DE UNA BOMBA DE CALOR A PARTIR DE LA ENERGÍA GEOTÉRMICA PARA ACONDICIONAR UN INVERNADERO FLORÍCOLA [Central University of Ecuador]. http://www.dspace.uce.edu.ec/handle/25000/18788.

Hafeez, M., Yuan, C., Shah, W.U.H., Mahmood, M.T., Li, X., Iqbal, K., 2020. Evaluating the relationship among agriculture, energy demand, finance and environmental degradation in one belt and one road economies. Carbon Manag. 11 (2), 139–154.

Hakvoort, G., Van Reijen, L.L., Van Aartsen, A.J., 1985. Measurement of the thermal conductivity of solid substances by DSC. Thermochim. Acta.

Hall, C.A., León-Pérez, C., Leclerc, G., 2000. Quantifying Sustainable Development: the Future of Tropical Economies. Academic Press, US, ditorial San Diego, CA. http://www.sidalc.net/cgi-bin/wxis.exe/?IsisScript=oet.xis&method=post&formato=2&cantidad=1&expresion=mfn=021995.

He, F., Zeng, L., Li, D., Ren, Z., 2019. Study of LED array fill light based on parallel particle swarm optimization in greenhouse planting. Inf. Process. Agric. 6 (1), 73–80.

Hermatian, A., Ajabshirchi, Y., Faramarz, S., Taki, M., 2019. An experimental analysis of a solar-assisted heat pump (SAHP) system for heating a semisolar greenhouse. Energy Sources, Part A Recovery, Util. Environ. Eff. 43 (14), 1724–1744.

IGSHPA, 2016. Closed-loop/geothermal heat pump systems. In: Design and Installation Standards. INTERNATIONAL GROUND SOURCE HEAT PUMP ASSOCIATION. https://geoconnectionsinc.com/resources/downloads/IGSHPA_Design_Installation_Standards_2016.pdf.

Instituto de Investigación Geológico y Energético, 2019. *Evaluación del recurso geotérmico de baja temperatura para el incremento de la productividad agrícola en invernaderos*. Evaluación Del Recurso Geotérmico de Baja Temperatura Para El Incremento de La Productividad Agrícola En Invernaderos. https://www.geoenergia.gob.ec/evaluacion-del-recurso-geotermico-de-baja-temperatura-para-el-incremento-de-la-productividad-agricola-en-invernaderos-2/.

Krausmann, F., Fischer-Kowalski, M., Schandl, H., Eisenmenger, N., 2008. The global sociometabolic transition: past and present metabolic profiles and their future trajectories. J. Ind. Ecol. 12 (5–6), 637–656.

Lahsen, A., Rojas, J., Morata, D., Aravena, D., 2015. Exploration for high-temperature geothermal resources in the andean countries of South America. World Geoth. Congr. 1996 (April), 19–25.

Lambert, J.G., Hall, C.A.S., Balogh, S., Gupta, A., Arnold, M., 2014. Energy. EROI Qual. Life 64, 153–167.

Lemmon, E.W., Jacobsen, R.T., Penoncello, S.G., Friend, D., 2000. Engineering Equation Solver. ASHRAE, p. 1993.

Li, C., Mao, J., Peng, X., Mao, W., Xing, Z., Wang, B., 2019. In Fl Uence of Ground Surface Boundary Conditions on Horizontal Ground Source Heat Pump Systems, 152, pp. 160–168 (September 2018).

Lloret, A., Labus, J., 2014. Geothermal Development in Ecuador: History, Current Status and Future. May, 11.

Long, T.B., Blok, V., Coninx, I., 2016. Barriers to the adoption and diffusion of technological innovations for climate-smart agriculture in Europe: evidence from The Netherlands, France, Switzerland and Italy. J. Clean. Prod. 112, 9–21.

Lund, J.W., Toth, A.N., 2021. Geothermics Direct Utilization of Geothermal Energy 2020 Worldwide Review, 90 (July 2020).

Marchi, B., Zanomi, S., Pasetti, M., 2019. Industrial symbiosis for greener horticulture practices: the CO2 enrichment from energy intensive industrial processes. Procedia CIRP 69 (May), 562–567.

Maripangui, R., Aravena, D., Garcia, K., Daniele, L., 2016. Assessment of geothermal heat pump heating systems in Coyhaique city , Chilean Patagonia. In: Proceedings 38th New Zealand Geothermal Workshop, November.

Miller, C., 2019. *Vegetable Operations Grow Indoors*. 2019 State of the Vegetable Industry Survey R. https://www.growingproduce.com/vegetables/55-of-vegetable-operations-grow-indoors-2019-state-of-the-vegetable-industry/.

Ministerio de Energía, 2017. *Bomba de calor geotérmica para climatización de invernadero*. Genera Tu Propia Energía. https://autoconsumo.minenergia.cl/?proyect_autoconsumo=bomba-de-calor-geotermica-para-climatizacion-de-invernadero.

Ministry of Agriculture, 2019. Agricultura, la base de la economía y la alimentación. https://www.agricultura.gob.ec/agricultura-la-base-de-la-economia-y-la-alimentacion/.

Nellis, G.F., Klein, S.A., 2009. Engineering Equation Solver. Cambridge University Press.

Nem, A., Nem, M., 2018. Analysis of the Possibilities of Using a Heat Pump for Greenhouse Heating in Polish Climatic Conditions — A Case Study.

Noorollahi, Y., Bigdelou, P., Pourfayaz, F., Youse, H., 2016. Numerical Modeling and Economic Analysis of a Ground Source Heat Pump for Supplying Energy for a Greenhouse in Alborz Province, Iran, 131, pp. 145–154.

Obara, S., Watanabe, S., Rengarajan, B., 2011. Operation method study based on the energy balance of an independent microgrid using solar-powered water electrolyzer and an electric heat pump. Energy 36 (8), 5200–5213.

OLADE, 2020. *Sistema de Información Energética de Latinoamérica y el Caribe - sieLAC*. Estadística Energética de América Latina y El Caribe. http://sielac.olade.org/WebForms/Reportes/SistemaNumerico.aspx?ss=2.

Payera, S.V., 2018. Geothermics Understanding social acceptance of geothermal energy : case study for Araucanía region , Chile. Geothermics 72 (March 2017), 138–144.

Pervanchon, F., Bockstaller, C., Girardin, P., 2002. Assessment of energy use in arable farming systems by means of an agro-ecological indicator: the energy indicator. Agric. Syst. 72 (2), 149–172.

Plante, A.F., Fernández, J.M., Leifeld, J., 2009. Application of thermal analysis techniques in soil science. Geoderma 153 (1–2), 1–10.

Pu, L., Xu, L., Qi, D., Li, Y., 2018. Structure optimization for horizontal ground heat exchanger, 136 (January), 131–140.

Roxer, M., Ritchie, H., 2019. *Hunger and Undernourishment*. Our World in Data. https://ourworldindata.org/hunger-and-undernourishment#citation.

Santos, A.F., Souza, H. J. L. De, Gaspar, P.D., 2016. Analysis of geothermal temperatures for heat pumps application in Paraná (Brasil). In: International Conference on Engineering 2015, pp. 485–491.

Stout, B., Fluck, R., 1992. Energy in World Agriculture. Elsevier.

United Nations, 2015. Sustainable development Goals. Sustainability. https://www.un.org/sustainabledevelopment/.

van Rijswick, C., 2018. World vegetable map 2018: more than just a local affair. In: *RaboResearch Food & Agribusiness* (Issue January). https://research.rabobank.com/far/en/sectors/regional-food-agri/world_vegetable_map_2018.html.

von Zabeltitz, C., 2011. Integrated greenhouse systems for mild climates. In: Integrated Greenhouse Systems for Mild Climates.

Widiatmojo, A., Chokchai, S., Takashima, I., Uchida, Y., Yasukawa, K., Chotpantarat, S., Charusiri, P., 2019. Ground-source heat pumps with horizontal heat exchangers for space cooling in the hot tropical climate of Thailand. Energies 12 (7), 1–22.

Willits, D.H., Peet, M.M., 1998. The effect of night temperature on greenhouse grown tomato yields in warm climates. Agric. For. Meteorol. 92 (3), 191–202.

Yang, W., 2021. Simulation study on the influence of roof inclination on the light environment of solar greenhouse. IOP Conf. Ser. Earth Environ. Sci. 621 (1).

Yao, Y., Xu, J., Sun, D., 2021. Untangling global levelised cost of electricity based on multi-factor learning curve for renewable energy : wind , solar , geothermal , hydropower and bioenergy. J. Clean. Prod. 285, 124827.

Yasutake, Daisuke, Tanioka, Hironobu, Ino, Aya, Takahashi, Akihiko, Yokoyama, Takayuki, Mori, Makito, Kitano, Masaharu, Miyauchi, Kiyoshi, 2017. Dynamic evaluation of natural ventilation characteristics of a greenhouse with CO2 enrichment. Acad. J. Agric. Res. 5 (October), 312–319.